J. Membrane Biol. 121, 101–117 (1991)
0022263191000060L

The Journal of
Membrane Biology

Topical Review

Liquid Junction Potentials and Small Cell Effects in Patch-Clamp Analysis

Peter H. Barry and Joseph W. Lynch
(with Appendix by Peter H. Barry)
School of Physiology and Pharmacology, University of New South Wales, Kensington, New South Wales 2033, Australia

Introduction

Since the early 1980s, the patch-clamp technique (Hamill et al., 1981) has been of particular value in investigating the properties of ion channels in cells. When used in either the intact or excised configurations, the properties of individual ionic channels can be directly measured. In addition, the whole-cell configuration can be used to investigate the total response of the full complement of channels in a cell. The whole-cell configuration is of particular value in exploring the properties of very small cells which are not readily accessible to conventional microelectrode techniques.

In all of the above measurements, there are two potential sources of error. In every situation there may be significant errors due to uncompensated junction potentials, which *may appear* to be eliminated by the normal zeroing procedure whereby residual potentials between pipette and bath solutions are offset prior to patch formation. In addition, in the intact and whole-cell patch configurations, the effect of the cells being small can introduce radical errors in the measurement of single-channel and whole-cell properties.

The aim of this review is firstly to outline the contribution of such junction potentials and the errors resulting from measurements on small cells and secondly to indicate how adequate junction potential corrections can be applied and the true values of underlying membrane parameters determined for such cells. Where necessary, appropriate equations have been presented. Much of the material is a review of published work. However, the review also seeks to extend the implications of that work and, in particular, it also includes (in an appendix) a time-dependent solution of the current relaxation following a channel closure.

Key Words patch clamp · single channels · liquid junction potentials · small cell effects

Patch-clamp Techniques Appear to Cover up Large Junction Potential Corrections

Whenever solutions with two different compositions come into contact, a liquid junction potential is developed between them. For example, as illustrated in Fig. 1, in normal intracellular measurements of cell membrane potentials, the *actual* membrane potential, E_m, of the cell is related to the *experimentally measured* value, V_e, by

$$E_m = V_e - (E_L^o - E_L^i) \tag{1}$$

where E_L^o and E_L^i represent the liquid junction potentials of the external and internal electrodes, respectively, in both cases being taken as that of bathing (or cell) solution with respect to electrode solution. Although there are some particular peculiarities of KCl junction potentials (Barry & Diamond, 1970), the advantage of (free-flowing) 3M KCl-filled microelectrodes derives from the fact that K^+ and Cl^- ions have similar (but unequal) mobilities and that there is a high concentration of KCl in the electrodes. The similarity of the mobilities results in the junction potentials being small, and the high concentration of the KCl solutions causes the electrode solution to dominate the junction potentials so that they are relatively independent of the solutions into which the electrode is placed. For typical external and internal cellular compositions, $(E_L^o - E_L^i) \approx 2.0$ mV, so that

$$E_m \approx V_e - 2.0\,\text{mV}. \tag{2}$$

For many electrophysiological situations, such a

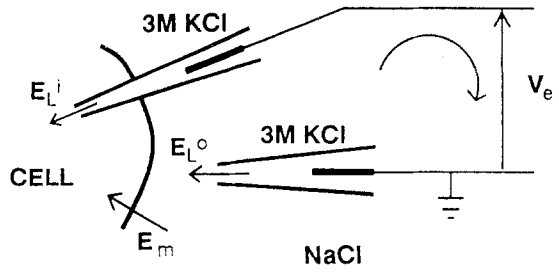

Fig. 1. The role of junction potentials in the measurement of the cell membrane potential when typical conventional microelectrodes are used. Applying Kirchoff's Loop rule in a clockwise direction as indicated: $-V_e + E_L^o + E_m - E_L^i = 0$, so that $E_m = V_e - (E_L^o - E_L^i)$, where E_m is the actual membrane potential, V_e is the experimentally determined value and E_L^i and E_L^o are the internal and external electrode liquid junction potentials, respectively, in both cases being measured (or calculated) in the direction of solution with respect to electrode. Typical internal and external cellular solution compositions and 3 M KCl-filled electrodes result in small junction potential corrections $(E_L^o - E_L^i)$ of the order of 2.0 mV, so that $E_m \approx V_e - 2.0$ mV

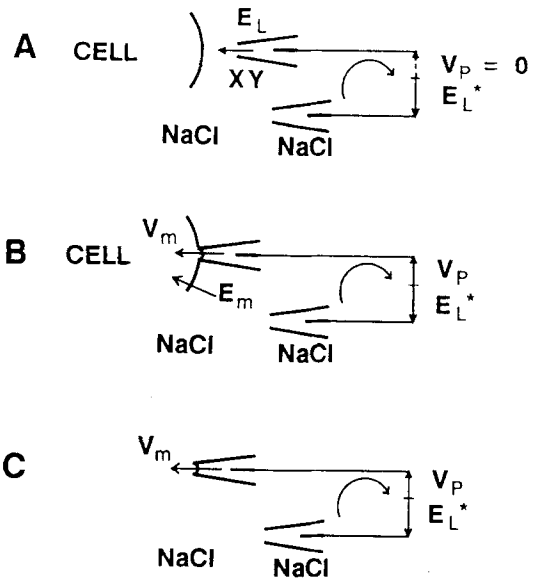

Fig. 2. The role of junction potentials in the measurement of intact and excised patch-clamp measurements (similar to Fig. 5 of Barry, 1989). (*A*) The initial situation prior to seal formation, in which the patch-clamp amplifier is zeroed and any imbalance in circuit potentials backed off. Using Kirchoff's Loop rule in a clockwise direction (as indicated) in *A*, $E_L^* - E_L = 0$. (*B*) With intact patches, the junction potential E_L has been replaced by the potential across the patch, V_m, but the backed off value, E_L^*, still remains. Hence, $E_L^* + E_m - V_m - V_P = 0$. Thus, the potential across the intact membrane patch is given by $V_m = (E_m - V_P) + E_L$. (*C*) With excised patches, the situation is the same as in *B*, but with $E_m = 0$. The potential V_m is normally defined as the solution (interior membrane surface) with respect to pipette for inside-out patches (as in figure), so that $V_m = -V_P + E_L$. For outside-out patches, defined as pipette (interior membrane surface) with respect to solution, V_m is replaced by $-V_m$, so that $V_m = V_P - E_L$

correction is relatively small and can often be neglected, especially if very precise values are not required.

However, in patch-clamp measurements the electrode solutions are at a very much lower concentration, being typically about 150 mmol · liter^{-1}. Under these conditions, solutions containing ions with significantly different mobilities (e.g., KF: $u_F/u_K = 0.753$; *see* Table 1 later) may readily generate junction potentials of up to about 10 mV, or possibly even more. Furthermore, in both single-channel and whole-cell patch-clamp measurements the presence of junction potentials is generally obscured. This occurs firstly because the procedure used to set up and zero the patch-clamp amplifier can give the impression that any junction potentials have been balanced out and secondly because in many patch-clamp situations the junction potential *seems* to disappear with seal formation. Although it is true that any imbalance in the actual electrode potentials will be balanced and remain so (*see* Discussion in Barry, 1989), it is not true of the junction potentials. Indeed, it should be stressed that under *no circumstances* is it possible to eliminate the junction potential correction by simply zeroing the patch-clamp amplifier (*see also* Neher, 1991). Apart from the trivial situation in which the solution composition of the pipette and bathing solution are the same, the liquid junction potential contribution to any measured potentials *never* disappears.

Figure 2 illustrates the principle for intact and excised patch-clamp configurations. Figure 2*A* shows the initial situation prior to seal formation with the patch electrode containing a solution of XY (i.e., X^+Y^-)^1 and the cell being bathed by a solution of NaCl. For simplicity, but without any loss of generality, since it will remain cancelled out, the NaCl reference electrode solution can be considered the same as the bathing solution. There will therefore only be one junction potential correction, E_L, (solution with respect to pipette) generated at the junction of the XY and NaCl solutions, that needs to be considered. When the amplifier is zeroed prior to seal formation, this junction potential, E_L, is balanced by an equal and opposite back-off potential, E_L^*, within the patch-clamp amplifier. This can readily be seen on application of Kirchoff's loop rule (e.g., Serway, 1986) in the direction indicated in Fig. 2*A*, since:

$$E_L^* - E_L = 0. \tag{3}$$

The junction potential illusion then arises as follows. Since the patch pipette is sealed against the cell

membrane (Fig. 2*B* and *C*) and the *XY*: NaCl junction potential, E_L, now disappears, being replaced by the potential, V_m, across the membrane patch, the impression is given that junction potential corrections are no longer necessary. However, the problem is that the back-off potential, E_L^*, that balanced the original junction potential is still present within the amplifier. For an intact patch or inside-out patch, V_m will be defined as cell solution (*S*; or interior membrane surface) with respect to pipette (*P*). In contrast, for an outside-out patch, it will be pipette (now interior membrane surface) with respect to solution.

Intact Patch Junction Potential

Hence, again applying Kirchoff's loop rule (Fig. 2*B*)

$$E_L^* + E_m - V_m - V_P = 0. \tag{4}$$

Hence, the potential, V_m, just across the membrane patch is therefore given by

$$V_m = (E_m - V_P) + E_L. \tag{5}$$

Excised Patch Junction Potential

In this case (Fig. 2*C*), a junction potential correction is still needed. In fact, Eq. (5) still applies (with $E_m = 0$). For an outside-out patch, V_m simply needs to be replaced by $-V_m$ in the above equations. For both situations V_m is given by

$$\begin{aligned} &\text{Inside-out patch} \quad && V_m = -V_P + E_L \\ &\text{Outside-out patch} \quad && V_m = V_P - E_L. \end{aligned} \tag{6}$$

For example, if $E_L = +5$ mV (solution − pipette), then Eq. (6) implies that for an *inside-out* patch (or intact patch), correction for the junction potential requires *adding 5 mV* to the uncorrected value of V_m; whereas for an *outside-out* patch 5 mV should be *subtracted* from it (*see*, e.g., Fenwick, Marty & Neher, 1982; Neher, 1991).

Whole-Cell Junction Potential

Even in the *whole-cell configuration* (Fig. 3), junction potential corrections are almost always required. Initially, prior to seal formation, the amplifier is zeroed (Fig. 3*A*) and using Kirchoff's rule again in the direction indicated

$$E_L^{o*} - E_L^o = 0 \tag{7}$$

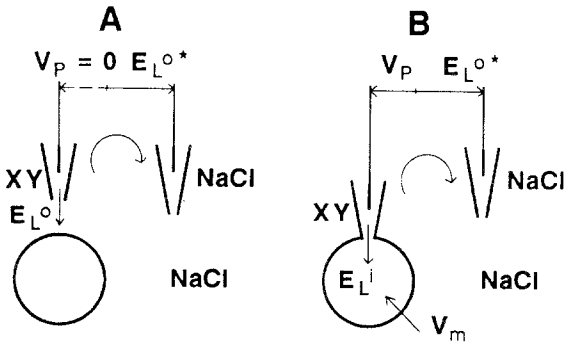

Fig. 3. Junction potentials in the whole-cell configuration. (*A*) The initial situation prior to seal formation, in which the patch-clamp amplifier is zeroed and any imbalance in circuit potentials backed off. From Kirchoff's rule, the back-off potential, $E_L^{o*} = E_L^o$, the liquid junction potential of the bath with respect to the pipette. (*B*) The whole-cell situation. E_L^o is replaced by E_L^i, which will tend to zero as the cell contents become dialyzed by the pipette contents. In such a situation, from Kirchoff's rule (in the direction indicated), $-V_P + E_L^{o*} + V_m - E_L^i = 0$, so that $V_m = V_P + E_L^i - E_L^o$. When the cell's contents are almost completely dialyzed, $E_L^i \approx 0$, and so, in such a case, $V_m = V_P - E_L^o$

so that a back-off potential, E_L^{o*}, exactly balances the initial external junction potential, E_L^o, of the bathing solution (e.g., NaCl) with respect to the pipette solution (X^+Y^-; *see* Footnote 1). When a seal is established and the patch ruptured, this junction potential is replaced by a new one, E_L^i, the junction potential of the internal solution of the cell with respect to the patch electrode, but, as before, the back-off potential, E_L^{o*}, still remains. Again from Kirchoff's rule, summing the potentials in the direction indicated in Fig. 3*B*

$$E_L^{o*} + V_m - E_L^i - V_P = 0 \tag{8}$$

so that from Eq. (8), using Eq. (7)

$$V_m = V_P + E_L^i - E_L^o. \tag{9}$$

If the cell volume is small compared to the pipette volume, and there is good solution exchange between the pipette and cell, the cell contents would be effectively dialyzed by the pipette solution. When this occurs, E_L^i would tend to zero and

$$V_m = V_P - E_L^o. \tag{10}$$

[1] Of course, it should be pointed out that even if the predominant anion in the pipette is not Cl^-, there ought to be some Cl^- present in the pipette so that the electrode potential remains stable and well defined [e.g., *see* Barry and Diamond (1970) for further discussion].

In this situation, if the junction potential for E_L^v ($E^S - E^P$) is +5 mV, then $V_m = V_P - 5$ mV (e.g., Fenwick et al., 1982; Neher, 1991).

Because of the presence of large relatively immobile anions, E_L^i is not just a simple liquid junction potential. As Marty and Neher (1983) point out, it is a Donnan potential, the cell interior being negative with respect to the pipette. Following their analysis, for the simple case where the pipette solution only contains univalent ion pairs (e.g., X^+Y^-), it may be shown that the "initial" peak value of E_L^i (after small mobile ions like K^+ and Cl^- have equilibrated, with an expected time course of seconds) will be given by:

$$E_L^i = (RT/F) \ln \{[(r^2 + 4)^{1/2} - r]/2\} \tag{11}$$

with

$$r = [A]_i/[X]_P$$

where $[A]_i$ represents the total initial concentration of large "immobile" anions in the cell and $[X]_P$ is the cation concentration in the pipette. For example if $[A]_i = [X]_P$ (i.e., $r = 1$), then this "initial" $E_L^i \approx -12$ mV and uncorrected voltage-dependent measurements will appear to be shifted in a depolarizing direction. As these "immobile" anions diffuse out of the cell, E_L^i will drop towards zero, with a time course of minutes. For further details, typical time courses (e.g., time constants of about 15 min for some cells), and experimental verification of this effect *see*, e.g., Marty and Neher (1983), Fernandez, Fox and Krasne (1984) and Pusch and Neher (1988).

Having determined the presence and sign of the regular junction potential corrections in a particular situation, it remains to evaluate their magnitude.

Two Questionable Procedures

1) It has been suggested that the initial measurement of the patch-clamp amplifier offset would give a measure of the liquid junction potential correction, which could be used for later adjustment of measurements. This would indeed only be valid if the two electrode potentials were exactly equal (for circuit contribution of electrode potentials, *see* Barry, 1989). Unfortunately, such electrode potential values are generally somewhat uncertain and unlikely to be exactly balanced.

2) It has also been suggested that zeroing the patch-clamp amplifier offset after gigaohm seal formation with a channel closed, prior to recording any measurements with the channel open, effectively balances any junction potentials and electrode potentials. However, this second procedure would only be valid under very restrictive conditions: if there were no nonzero diffusion potentials across the rest of the patch and if the seal resistance were effectively infinite. These conditions seldom, if ever, exist.

The Magnitudes of Junction Potentials in Different Solutions

The magnitudes of junction potentials can be determined either by measuring them experimentally or by calculating them. Because potential measurements always require two electrodes, the procedure requires various assumptions and is not generally very equivocal. Therefore, it is often simpler to calculate liquid junction potentials using an equation such as the generalized Henderson Liquid Junction Potential Equation.[2] For N polyvalent ions, the potential E of solution (S) with respect to pipette (P) is given by

$$E^S - E^P = (RT/F)S_F \ln \left\{ \sum_{i=1}^{N} z_i^2 u_i a_i^P \Big/ \sum_{i=1}^{N} z_i^2 u_i a_i^S \right\} \tag{12}$$

where

$$S_F = \sum_{i=1}^{N} [(z_i u_i)(a_i^S - a_i^P)] \Big/ \sum_{i=1}^{N} [z_i^2 u_i (a_i^S - a_i^P)]$$

where u, a and z represent the mobility, activity and valency (including sign) of each ion species (i). Although such a generalized equation is of very general value since it can readily cater for any combination of salts, it may only give an approximate estimate of junction potential values in some situations because its underlying assumptions are not always very well defined electrochemically.

However, in certain situations, Eq. (12) can be considerably simplified, is very much better defined and predicts values in fairly close agreement with carefully determined experimental

[2] This equation (*cf.* MacInnes, 1961) was originally modified (Barry & Diamond, 1970) to include activities rather than just concentrations on the assumption that the ions obey the Guggenheim condition [i.e., that the individual ion activity coefficients of each ion are equal at every point, so that $\gamma_1(x) = \gamma_2(x) = \gamma_3(x) = \ldots = \gamma(x)$]. Since then it has also been extended to its form in Eq. (12) to allow for the possible inclusion of polyvalent ions (e.g., Morf, 1981; Ammann, 1986).

measurements (e.g., Barry & Diamond, 1970; Barry, 1989).

For example, for a simple dilution situation with monovalent ions (e.g., NaCl[150] : NaCl[75]), the equation becomes

$$E^S - E^P = \frac{RT}{F}\frac{(u_+ - u_-)}{(u_+ + u_-)} \ln\left\{\frac{a^P}{a^S}\right\} \tag{13}$$

where u_+ and u_- are the relative mobilities of the cations and anions, which are both assumed to have the same activity coefficients ($\gamma_+ = \gamma_-$; the Guggenheim assumption).

Alternatively for a simple biionic situation with only monovalent ions (e.g., NaCl[150] : KCl[150]), the equation becomes

$$E^S - E^P = \frac{RT}{F}\frac{[a^S(u_+^S - u_-^S) - a^P(u_+^P - u^P)]}{[a^S(u_+^S + u^S) - a^P(u_+^P + u^P)]} \cdot \ln\left\{\frac{[a^P(u_+^P + u^P)]}{[a^S(u_+^S + u^S)]}\right\}. \tag{14}$$

If $a^P = a^S$, this equation simplifies even more radically, reducing to the equivalent Planck equation, to give

$$E^S - E^P = \frac{RT}{F} \ln\left\{\frac{(u_+^P + u_-^P)}{(u_+^S + u_-^S)}\right\}. \tag{15}$$

Further details of such junction potential calculations are given by MacInnes (1961), Caldwell (1968), Barry and Diamond (1970), Page (1980), Morf (1981), Ammann (1986) and Barry (1989). A list of some of the more common absolute ionic mobilities (relative to K^+) is given in Table 1. These values have been calculated from measurements of limiting equivalent conductance Λ^0 [since the absolute mobility u is equal to $\Lambda^0/(|z_i|F^2)$]. Values of Λ^0 and activity coefficients are listed for many ions in Robinson and Stokes (1965), Meier et al. (1980) and Dean (1985). If published values of mobilities cannot be obtained, either they may have to be directly evaluated by means of measuring their limiting equivalent conductance (*see also* conductance measurements in Weast, 1980) or else an attempt made to measure the liquid junction potential itself (e.g., Barry & Diamond, 1970; Page, 1980, and in particular for patch clamp measurements, *see* Neher, 1991).

Values of liquid junction potentials for some solutions are listed in Table 2 (*see also* Barry & Diamond, 1970; Barry, 1989). Although ion activities should be used for very accurate estimates, the table clearly indicates that in most situations, calculations using concentrations provide an adequate estimate of the liquid junction potential. For example, for the worst case given in the table for the solutions with known activity coefficients, LiCl 150 : KCl 150, the error in using concentrations is only 0.1 mV. Where activity coefficients differ even more radically between solutions, as may well be the case with some large organic ions, the differences will become significant. In general, it should be noted from Table 2, that lower concentrations of pipette solutions in patch-clamp measurements, and the inclusion of ions like choline, result in junction potentials of greater magnitude than those generally experienced in other microelectrode measurements in electrophysiology.

In addition, further practical information about junction potential corrections in patch-clamp measurements may be found in a recent chapter by Neher (1991), which, in addition, clearly describes the measurement of junction potential values in the patch-clamp situation.

Patch-clamp Measurements on Small Cells Require Large Corrections

The patch-clamp technique has enabled the detailed electrophysiological characterization of small cells that were previously inaccessible to intracellular microelectrode impalement. However, this technique has limitations in both the cell-attached and whole-cell modes when studying cells with whole-cell resistances (R_o) in the order of gigaohms. There is strong evidence that many types of electrically excitable and inexcitable cells have whole-cell resistances in this range. For example, isolated pancreatic β-cells (10–15 μm diameter) have input resistances of at least 20 GΩ, as verified by both electrophysiological (Rorsman & Trube, 1986) and tracer flux (Atwater, Rosario & Rojas, 1983) measurements. The highest reported values of R_o seem to be in mammalian T-lymphocytes (6–8 μm diameter), which have peak values of 100 GΩ (Cahalan et al., 1985). Mammalian olfactory receptor neurons ($\approx$8 μm diameter), which we use as a model small cell, have calculated whole-cell resistances of 20–30 GΩ (Lynch & Barry, 1989, 1991). These values are as would be predicted from much larger amphibian olfactory receptor neurons ($R_o \approx 5$ GΩ: Trotier, 1986; Firestein & Werblin, 1987; Frings & Lindemann, 1988; Dionne, 1989; Schild, 1989; Suzuki, 1989) when differences in cell size are taken into account. Numerous other examples of cell types with gigaohm resistances have been reported, and many of these have been measured by techniques which underestimate the true R_o.

Table 1. Absolute ionic mobilities (u_X/u_K) relative to K^+ at 25°C for various ions (X)[a]

X	u_X/u_K	X	u_X/u_K	X	(u_X/u_K)
H^+	4.759[b]	Ca^{2+}	0.4048[b]	NO_3^-	0.972[b]
Rb^+	1.059[b]	Mg^{2+}	0.361[b]	ClO_4^-	0.916[b]
Cs^+	1.050[b]	Sr^{2+}	0.404[b]	$Acetate^-$	0.556[b]
K^+	1.000[b]	Ba^{2+}	0.433[b]	HCO_3^-	0.605[c]
Ag^+	0.842[b]	Be^{2+}	0.31[b]	SCN^-	0.90[c]
Na^+	0.682[b]	Cu^{2+}	0.365[b]	$Picrate^-$	0.411[c]
Li^+	0.525[b]	Zn^{2+}	0.359[b]	$Propionate^-$	0.487[c]
NH_4^+	1.000[b]	Co^{2+}	0.37[b]	$Sulfonate^-$	0.586[c]
Tl^+	1.033[c]	Pb^{2-}	0.473[b]	$Lactate^-$	0.528[c]
TMA[d] $[N(CH_3)_4^+]$	0.611[b]	La^{3+}	0.316[b]	$Benzoate^-$	0.441[c]
TEA[d] $[N(C_2H_5)_4^+]$	0.444[b]	OH^-	2.698[b]	$H_2PO_4^-$	0.45[c]
TPrA[d] $[N(C_3H_7)_4^+]$	0.318[b]	F^-	0.753[b]	HPO_4^{2-}	0.39[c]
TBuA[d] $[N(C_4H_9)_4^+]$	0.264[b]	Cl^-	1.0388[b]	SO_4^{2-}	0.544[b]
TAmA[d] $[N(C_5H_{11})_4^+]$	0.237[b]	Br^-	1.063[b]		
Choline $[NC_7H_{16}]$	0.48[e]	I^-	1.045[b]		

[a] The absolute ionic mobility (u_X) was obtained from the limiting equivalent conductance (Λ^0), since $u_X = \Lambda^0/(|z|F^2)$, where z is the valency of the ion. The number of significant figures reflects the number given in the original limiting equivalent conductance data.

[b,c] Obtained from Λ^0 data in Robinson and Stokes (1965)[b] and Dean (1985)[c].

[d] TMA represents tetramethylammonium$^+$; TEA, tetraethylammonium$^+$; TprA, tetra-*n*-propylammonium$^+$; TBuA, tetra-*n*-butylammonium$^+$ and TAmA, tetra-*n*-amylammonium$^+$.

[e] Estimated by interpolation from above TMA, TEA etc., Λ^0 data in Robinson and Stokes (1965) on the basis of carbon chain length.

The seal resistance (R_s) between the cell membrane and the glass pipette generally does not exceed 50 GΩ (Fischmeister, Ayer & DeHaan, 1986). For large cells this is orders of magnitude greater than the whole-cell resistance (R_o) and its contribution to the whole-cell conductance can be neglected. However, for small cells with input resistances in the order of gigaohms, the contribution of R_s to the whole-cell conductance does become significant. The usual method of determining R_o by measuring the change in current in response to voltage steps in these cells can yield significant errors. For example, for an R_o of 20 GΩ and an R_s of 30 GΩ, the apparent whole-cell resistance (R_{app}) is 12 GΩ, which represents a 40% error. Also, because R_s is similar in magnitude to R_o, it represents a relatively low resistance pathway to ground, thus tending to short-circuit the resting potential of the cell. Hence measured cell resting potentials are also significantly underestimated in these cells.

For cell-attached patches on large cells, current passing through open channels or through the patch leakage resistance (R_p) has an insignificant effect on the membrane potential because of the extremely low current density flowing across the rest of the cell. In such cases, the cell membrane is very well voltage-clamped, the membrane potential of the cell remaining constant as pipette potential is varied. Thus, any channel opening to a single conductance level will result in a well-defined rectangular current waveform and channel conductances and correct values of reversal potentials can be measured directly. This large-cell requirement for adequate voltage clamping has been appreciated since the first gigaohm seal patch-clamp measurements were made (Hamill et al., 1981). However, the situation is very different in cells with gigaohm input resistances. Because R_p is usually less than would be predicted from the area of the patch and in small cells is often similar in magnitude to R_o (Fenwick et al., 1982; Fischmeister et al., 1986; Lynch & Barry, 1989), simply varying the pipette potential can change the membrane potential, resulting in large errors in the measurement of single-channel conductances and reversal potentials. Also, because the resistances of single channels are often of similar magnitude to the whole-cell resistance, the opening and closing of single channels can cause significant changes in the membrane potential, thereby distorting the shape of single-channel current waveforms. In this section, we present several methods of estimating corrected values of R_o from data obtained in the whole-cell and cell-attached patch-clamp configurations and show how measurements of single-channel conductance and reversal potential can be corrected for the small size of the cell.

Table 2. Examples of some liquid junction potentials calculated with the Generalized Henderson Equation [Eqs. (11) and (12)] for some typical simplified patch-clamp solutions[a]

Solution (S) (mmol · liter^{-1})	Pipette (P) (mmol · liter^{-1})	Potential ($E^S - E^P$) (mV)
NaCl 150	KCl 150	+ 4.3[b]
LiCl 150	KCl 150	+ 6.8 [+ 6.7[c]]
CsCl 150	KCl 150	− 0.6[b]
RbCl 150	KCl 150	− 0.7[b]
NaCl 150	CholineCl 150	− 3.2[d]
NaCl 150	NaF 150	+ 4.6[b]
NaCl 150	KF 150	+ 8.8[b]
CholineCl 150	KF 150	+ 12.5[d]
TEACl 50 + NaCl 100	NaCl 150	+ 1.2[d]

[a] They were calculated using the appropriate values of ionic mobilities (u_X/u_K) listed in Table 1. Except where stated, concentrations were used in the calculations. In all but one case (LiCl : KCl, as indicated), where activity coefficients were available, the potential calculated from activities agreed with the value calculated from concentrations to within the accuracy specified. When required, the activity was calculated using the activity coefficients obtained from the tables in Robinson and Stokes (1965).
[b] Concentration and activity calculations agreed within accuracy specified.
[c] Calculated using activities.
[d] Calculated only using concentrations, in absence of activity data.

How to Recognize a High Whole-Cell Resistance (R_o)

Firstly, it is reasonable to suspect that any cell with a diameter of <15 μm without significant arborizations may have an R_o in the order of gigaohms. In the whole-cell configuration, additional indications may be that:

1) R_{app} (the apparent or measured value of whole-cell resistance) is in the gigaohm range. If R_{app} is in this range, then R_o may be much higher.
2) Measured membrane potentials are unrealistically low (e.g., too low to generate a spike).
3) Cells with a low R_{app} (because of a low R_s) have measured resting potentials close to zero.
4) There is reduced sensitivity to the application or removal of series resistance compensation (either to the speed of the voltage-clamp or to the magnitudes of peak currents).

In the cell-attached configuration, the most reliable indication is that the opening of single channels can cause a dramatic increase in the cell spiking rate (Fenwick et al., 1982; Ashcroft, Harrison & Ashcroft, 1984; Maue & Dionne, 1987; Frings & Lindemann, 1988; Kehl & McBurney, 1989; Lynch & Barry, 1989; Trotier, Rosin & MacLeod, 1989) because the current flowing across the patch is able to depolarize the cell to the action potential threshold. The resultant action potential in the rest of the cell then induces a biphasic current waveform, with both capacitative and resistive components, across the patch (e.g., Fig. 4*A* and *D*). Other indications may be:

1) The appearance of exponential relaxations on single-channel current transitions (e.g., Fig. 4*B* and *C*).
2) Lower channel conductances in cell-attached rather than excised patches (Fischmeister et al., 1986; Lynch & Barry, 1989).
3) Unexpectedly nonlinear conductances in cell-attached patches, caused by R_o varying with membrane potential.
4) Spikes initiated by current injection through R_p (Fig. 4*D*).

The regular appearance of any or all of these effects strongly suggest a high R_o and indicate that corrections need to be applied to obtain corrected values of R_o, single-channel conductances and reversal potentials.

Estimation of R_o in the Whole-cell Patch-clamp Configuration

In the whole-cell recording configuration (Fig. 5*A*), the pipette solution is in direct contact with the internal environment of the cell, and in small cells, the cell solution is rapidly dialyzed (Marty & Neher, 1983). Apart from liquid junction potentials discussed earlier, there are two sources of error that must be considered. These errors are due to the series resistance (R_{sp} generally 1–20 MΩ) and the seal resistance (R_s generally 5–100 GΩ), respectively. In large cells where $R_o \ll R_s$, only series resistance errors need to be considered. *See* Sigworth (1983) for the theory and Marty and Neher (1983) for the practice of electronic series resistance compensation in large cells. In the absence of compensation, the maximum error in V_P is $i_P \cdot R_{sp}$, where i_P is the peak current in the pipette. In small cells, although series resistance errors are generally smaller because i_P is smaller, they may still be very significant. However, the whole-cell capacitance (C_o) is often small enough to make the voltage-clamp time constant ($R_{sp} \cdot C_o$) approach the time constant of the compensation circuit, thereby limiting the maximum fraction of compensation that is applied by such a circuit (Sigworth, 1983). Thus in very small cells, there can be a reduced ability to use such circuitry to electronically compensate for voltage errors due to current flow through the pipette.

In small cells, where R_o is comparable in magnitude to R_s (or greater than it), other errors become considerable. A simplified diagram of the whole-cell patch configuration is given in Fig. 5*B*. Series

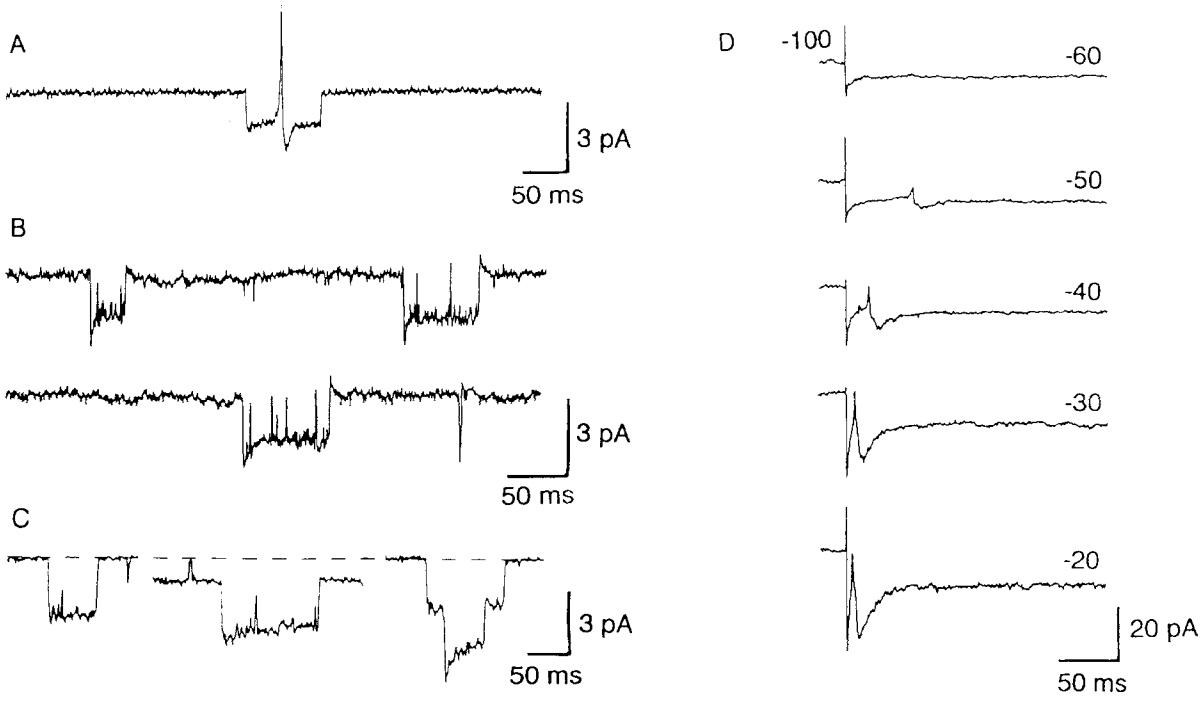

Fig. 4. Examples of small cell effects in cell-attached patches on enzymatically dissociated rat olfactory receptor neurons. For cell preparation and other experimental details, *see* Lynch and Barry (1989). Data were recorded from four different cells, each with high $[K^+]$ solution in the patch pipette. (*A*) Spike induced by the opening of a single 29-pS channel injecting current into the cell. The pipette potential was +70 mV. (*B*) Exponential current relaxations associated with the opening and closing of a 130-pS Ca^{2+}-activated K^+ channel. Pipette potential was +20 mV. (*C*) Demonstration of the effect of reducing R_P on 'on' relaxation time constants (τ^{on}). The opening of a 52-pS K^+ channel is shown from the baseline (left), superimposed on a 29-pS channel (center) and superimposed on another 52 pS K^+ channel (right). Note the progressive decrement of 'on' time constants. The absence of significant 'off' relaxations implies a high R_P (and/or possibly high C_P). The pipette potential was +40 mV. (*D*) An example of current injection through R_P depolarizing the cell to spike threshold. The pipette potential was held at −100 mV, then stepped to potentials from −60 to −20 mV in 10-mV increments. As current through R_P was increased, latency to action potential initiation was reduced

resistance has been neglected. Total current flowing into the amplifier (i_T) is given by

$$i_T = (V_P - E_s)/R_s + (V_P - E_o)/R_o \tag{16}$$

where V_P is the pipette potential, E_s is junction potential between external and internal (pipette) solutions and E_o is the zero-current resting membrane potential.[3] This situation is plotted in Fig. 5*B*. The slope of the line is given by:

$$\Delta i_T/\Delta V_P = 1/R_s + 1/R_o. \tag{17}$$

In large cells, because $R_s \gg R_o$, this slope provides a very close approximation to $1/R_o$. However, in small cells the current, i_s, flowing across R_s cannot be neglected because it represents a significant fraction of i_T. If the *I-V* relationship is extended to the point where $V_P = 0$, then the corresponding current (i_T^o) is given by

$$i_T^o = -E_s/R_s - E_o/R_o. \tag{18}$$

If $E_s \approx 0$ (i.e., the leakage potential between pipette and bath solutions, equivalent to a liquid junction potential across the seal, is negligible) then the equation reduces to

$$i_T^o = -E_o/R_o. \tag{19}$$

If it is assumed that in the region of greatest whole-cell resistance that the membrane is permeable only to K^+ ions, then E_o equals E_K, the K^+ equilibrium potential, and R_o can be determined. This enables R_s to be obtained from the slope of the *I-V* relation

[3] In order to make the equations and derivation more readable and uniform, the zero-current resting membrane potential of the cell (defined in Lynch and Barry (1989) as E_m) has now been defined as E_o (cf. R_o and C_o resistance and capacitance of the rest of the cell). Similarly, the diffusion potential across the patch (defined in Lynch and Barry (1989) as E_D) is now defined as E_p (*cf.* patch resistance R_p).

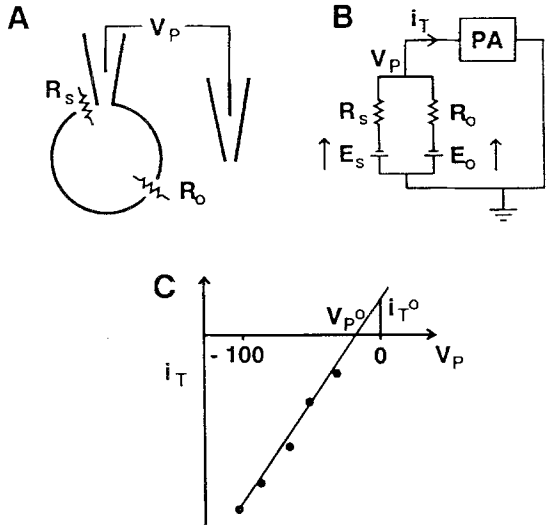

Fig. 5. The importance of the seal resistance in whole-cell measurements. (*A*) A schematic diagram of the experimental set-up. R_s and R_o represent the seal resistance and the whole-cell resistance, respectively. (*B*) The full circuit diagram of the set-up shown in *A*. E_s represents a possible junction potential across the seal resistance and E_o the zero-current resting membrane potential of the cell, both defined in the directions of the arrows; R_s and R_o are the same as in *A*; V_P represents the pipette potential and i_T the total current being measured by the patch-clamp amplifier (*PA*). (*C*) The relationship between i_T and V_P. i_T^o represents the total current at zero pipette potential, and V_P^o the pipette potential for which the total current is zero

[Eq. (17)]. If the liquid junction potential, E_s, is non-zero, then R_s and R_o can both be found by simultaneously solving Eqs. (17) and (18).

Then, in order to correct for liquid junction potentials, as discussed earlier, it is simply necessary to substitute $[V_P - (E_L^o - E_L^i)]$ for V_P, or $[V_P - E_L^o]$ for V_P if $E_L^i \approx 0$, in Eq. (16), where E_L^o and E_L^i are as defined in Fig. 3 [*cf.* Eqs. (9) and (10)]. To find i_T^o, the current should simply be determined as that value when $V_P = E_L^o - E_L^i$ (or $V_P \approx E_L^o$, if $E_L^i \approx 0$).

In principle at least, the hypothesis that $E_o \approx E_K$ can easily be tested. If, for example, a significant resting Na^+ conductance is suspected, the above analysis should be performed first in choline solution, then in Na^+ solution, and the slopes of the peak *I-V* relationships compared. If R_s is assumed to be essentially independent of solution composition (Fischmeister et al., 1986), then any change in R_o will be reflected by a change in the slope and can easily be calculated. Clearly, the proportionate decline in R_o in Na^+ solution gives an indication of the relative contribution of Na^+ to the resting conductance.

Care should be taken when measuring *I-V* relationships, since the opening and closing of single channels can cause significant changes to the whole-cell resistance. Also, since solution exchange sometimes damages the recording configuration, it is necessary to re-measure the *I-V* relationship in control solution afterwards. In practise, these methods give only an estimate of R_o and it may be necessary to average results from a number of cells (an example of such an analysis is given in Lynch & Barry, 1991).

Estimation of Whole-Cell Resistance (R_o) in Cell-Attached Patches

The electrical situation in a cell-attached patch is more complicated because both patch and cell electrical properties must be considered (Fig. 6). Consequently, there are a greater number of factors complicating the analysis of data recorded in this configuration. But as will be shown below, obtaining valid estimates of R_o and R_p is not difficult.

In any cell, the apparent (chord) conductance of the channel (γ_{app}) can be determined by measuring the change in current (Δi_T) measured during the opening of the channel at a patch potential (V_P) and resting cell membrane potential (E_o). It can be shown to be given by

$$\gamma_{app} = -\Delta i_T/(V_P - E_o + E_{app}) \tag{20}$$

where E_{app}, the apparent reversal (null) potential of the channel, is given by

$$E_{app} = E_o - V_P^o \tag{21}$$

and V_P^o is the value of the patch potential at which $\Delta i_T = 0$. Similarly, the (slope) conductance of the channel (γ_{app}) can be estimated from

$$\gamma_{app} = -d(\Delta i_T)/dV_P \tag{22}$$

without having to evaluate E_{app}. If the *I-V* relationship is linear, then both chord and slope conductances measured by Eqs. (20) and (22) will be equal. Any junction potential corrections can be made by substituting $V_P - E_L$ for V_P in Eqs. (20) and (21), where E_L is the liquid junction potential (solution – pipette; *see* Fig. 2).

For ideal large cells, the true channel conductance (γ_c) equals γ_{app} and the true reversal potential of the channel (E_c) equals E_{app}. Implicit in these equalities are two assumptions: (i) that $R_p \gg R_o$, implying that changing the pipette potential will have no effect on the internal potential of the cell, and (ii) that $R_c \gg R_o$, implying that single channels opening

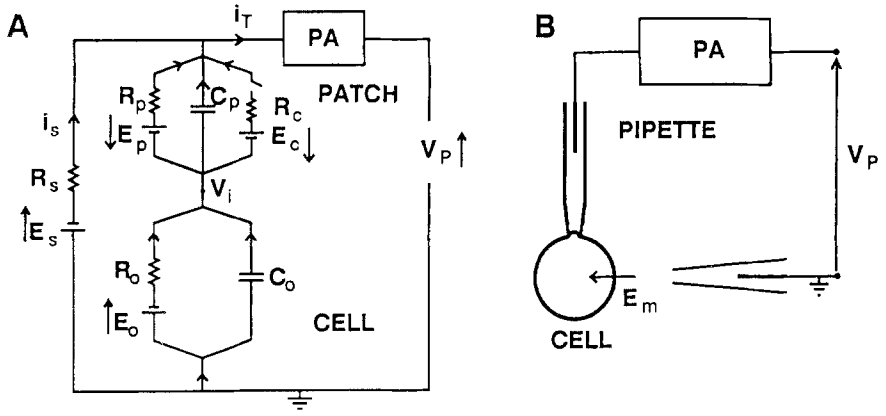

Fig. 6. (*A*) The equivalent electrical circuit of a small cell and membrane patch (with a channel that can be in either an open or a closed state; based on Fig. A1 of Lynch and Barry (1989), which was similar to one in Fenwick et al. (1982), with the addition of E_p and C_p in the patch and the leakage resistance of the seal R_s) for the circuit that is shown in *B*. *PA* refers to the patch-clamp amplifier; subscript p to the membrane patch; c to the channel resistance; s to the seal around the patch pipette and o to the rest of the cell. E_o represents the resting potential of the cell; E_p the diffusion potential across the patch; E_c the null potential of the channel in the patch; V_P the potential applied to the patch pipette and V_i the potential of the cell interior with respect to the external solution. R_c represents the resistance of the single channel (with conductance, γ_c) and R_s the pipette-seal resistance. The currents are defined as positive if in the same directions as the arrows in the diagram. (*B*) The experimental set-up for patch clamp measurements on an intact membrane patch (with symbols as in *A*)

in the patch will not be able to inject sufficient current into the cell to change the membrane potential. For small cells, with R_o in the gigaohm range, neither of these assumptions is valid and such equations are quite inadequate (Neher, Sakmann & Steinbach, 1978; Fenwick et al., 1982; Fischmeister et al., 1986: Lynch & Barry, 1989). The current flowing through the channel in the patch (R_c) or through the remaining area of the patch (R_p) can change the membrane potential so that E_o is no longer constant and equal to its value before the channel opened or before the pipette potential was changed. Examples of the types of effects this can produce are shown in Figs. 4, 7 and 8. In Fig. 7, the theoretical behavior of a 50-pS K^+-selective channel opening in a cell-attached patch is shown for representative values of R_o, R_p and V_P, and the magnitude of waveform distortion is shown to be very dependent on the ratio R_o/R_p.

If the initial peak value of the single-channel current is used before time-dependent relaxations take effect, it may be shown [Eq. (A17) in the Appendix: *see also* Lynch & Barry, 1989] that the single-channel conductance is given by

$$\gamma_c = -\Delta i_T/\{[(V_P - E_o - E_p\delta)/(1+\delta) + E_c][C_o/(C_o + C_p)]\} \quad (23)$$

where $\delta = R_o/R_p$; C_o and C_p are the capacitances of the cell and patch, respectively; E_p is the patch diffusion potential (cell with respect to pipette solution; Fig. 6) and E_c is the channel reversal potential given [*see* Eq. (A42) in the Appendix] by

$$E_c = (E_o + E_p\delta - V_P^o)/(1+\delta) \quad (24)$$

where, as before, V_P^o is the pipette potential for which the single-channel current, i_T, is zero. As illustrated, for example, in Fig. 7, δ (the ratio R_o/R_p) can have a dramatic effect on the reversal potential of channels in a small cell. Now, combining Eqs. (23) and (24) yields

$$\gamma_c = -\{\Delta i_T/(V_P - V_P^o)\} \cdot \{[1+\delta][1 + (C_p/C_o)]\} \quad (25)$$

and even if the following slope conductance equation is used

$$\gamma_c = -\{d(\Delta i_T)/dV_P\} \cdot \{[1+\delta][1 + (C_p/C_o)]\}. \quad (26)$$

Theoretically, the ratio C_p/C_o is equal to the ratio of the patch to the whole-cell membrane surface areas. Sakmann and Neher (1983) found that although C_p varied widely, measured values were not significantly different from those predicted by measuring pipette tip internal diameters. Accordingly, if pipette tip diameters are chosen to be small in comparison to the cell diameter, then C_p/C_o can be assumed to be zero, and the previous equation reduces to

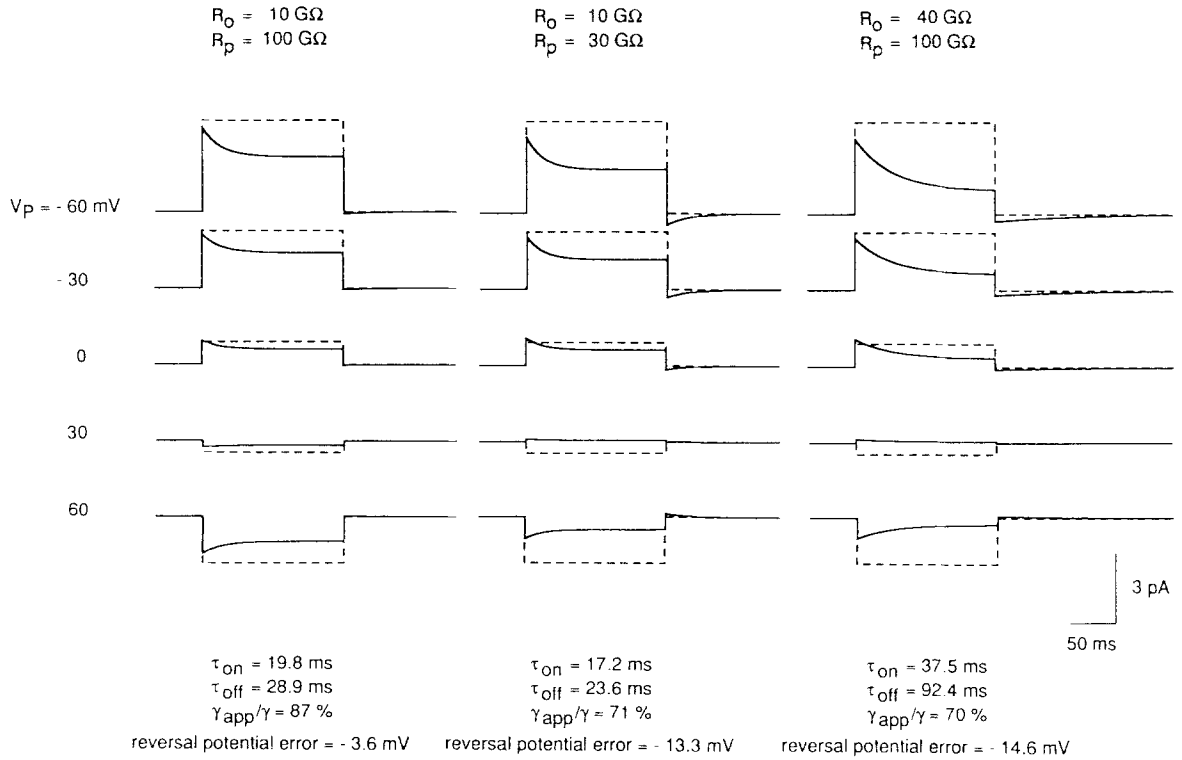

Fig. 7. The theoretical behavior of a 50-pS K^+-selective channel in a cell-attached patch for indicated values of R_o, R_p and V_P. The pipette was assumed to contain NaCl solution. The channel was assumed to be nonrectifying to illustrate both the changes in reversal potential and the independence of the small cell effects on the direction of current flow. The traces were directly printed on an HPLaserJet printer by a computer program using the equations in the appendix (*see* Appendix for parameter definitions, derivation of the mathematical model and computational details). Each trace commences with the channel in the closed state and upward transitions represent current flow out of the cell. The dashed lines represent the theoretical single channel currents expected for an infinitely large cell (i.e., $R_o/R_p \to 0$ and $C_p/C_o \to 0$). Values of R_o, R_p and V_P are shown for each continuous trace. Other parameters are: $E_o = -70$ mV, $E_p = -50$ mV, $E_c = -80$ mV, $C_o = 3$ pF and $C_p = 0.15$ pF. The value of E_p was chosen to reflect the predominately K^+ selective nature of the membrane, but with some nonselective leakage due to slight damage caused by the pipette. Some parameters affected by changes in R_o and R_p are shown beneath each set of traces. It may be seen that the relative values of R_o and R_p determine the magnitude of the current waveform distortion, whereas their absolute magnitudes determine the time constants for current relaxation

$$\gamma_c \approx \gamma_{app}(1 + \delta) = \gamma_{app}(1 + R_o/R_p) \quad (27)$$

where γ_{app} is the apparent cell-attached conductance, calculated by measuring the change in peak (initial) single-channel current as pipette potential is varied. Voltage ramps should not be used to measure γ_{app} because membrane potential changes lag pipette potential changes by up to several hundred milliseconds. Note also that, since R_o often declines with depolarization, γ_{app} may increase as pipette potential is increased and the cell is depolarized.

To determine R_o in cell-attached patches, it is also necessary to determine R_p. The resistance found by measuring the change in baseline current as the pipette potential is varied, represents the parallel sum of R_s and R_p and is often a poor estimate of R_p. Several other methods of estimating R_p exist. Fischmeister et al. (1986) used two patch electrodes to precisely determine R_p. Cell internal potential, controlled with one pipette in the whole-cell mode, was varied and current flow across another pipette, in cell-attached configuration on the same cell cluster, was directly measured. This gave precise and direct measurements of R_p, but is clearly impractical for routine use, particularly on isolated small cells. Fenwick et al. (1982) zeroed the current flow through R_s by using identical pipette and bathing solutions and holding pipette potential at 0 mV. Thus, by measuring the steady-state current flow out of the pipette in a cell-attached patch, and with knowledge of the membrane potential, R_p could be calculated. However, as noted by the authors, in small cells current flow through R_p may have substantially (and unpredictably) depolarized the cell, resulting in an overestimate of R_p. Lynch and Barry (1989) used a more complex means of estimating R_p and R_o, based on

analysis of cell excitability in response to channels opening in the patch. Below we describe two other more generally applicable methods of estimating R_p and R_o from single-channel data in a cell-attached patch.

Measurement of Exponential Current Relaxations

In the cell-attached configuration, stepwise current transitions often display exponential relaxations which occur because the current passing through the channel can depolarize (or hyperpolarize) the cell (Figs. 4, 7 and 8). It can be shown [Eqs. (A28) and (A29) in the Appendix], that

$$\tau_{on} = R_o(C_o + C_p)/(1 + R_o/R_p + R_o\gamma_c) \quad (28)$$

$$\tau_{off} = R_o(C_o + C_p)/(1 + R_o/R_p). \quad (29)$$

If the C_p term is ignored, these equations revert to those derived by Fenwick et al. (1982). If γ_c is measured directly in excised patches then R_o/R_p can be calculated from intact patch measurements of γ_{app} from Eq. (27). Typical values of C_o can be measured in the whole-cell recording configuration (Marty & Neher, 1983) and corrected for cell size. R_o can then be estimated from either Eq. (28) or (29). In practise, τ_{on} and τ_{off} are usually difficult to measure precisely although signal-to-noise ratio may be improved by averaging multiple events. It should be noted that τ_{off} normally has a much smaller amplitude than τ_{on} (e.g., Fig. 4*C*, Fig. 7) and is thus more difficult to measure. However, using the data displayed in Fig. 8, Fenwick et al. (1982) were able to deduce R_o and R_p from the measured values of τ_{on} and τ_{off} substituted into equations similar to Eqs. (28) and (29). Alternatively, if τ_{on} can be determined for two different conductance channels in the same patch or for the superpositioning of two similar channels (with R_p changed by the parallel addition of another $1/\gamma_c$ resistance; e.g., Fig. 4*C*), then R_o and R_p can be estimated by simultaneously solving the two sets of time constant equations generated.

Measurement of Proportionate Relaxation of Single-Channel Currents

To use this technique, it is necessary to have long open times so that steady-state current levels can be measured. Provided $C_p/C_o \ll 1$ and R_o/R_p is significant, it is possible to obtain estimates of R_o and R_p from the equations

$$i_{rel}^{off} \equiv \Delta i_T^*(0)/\Delta i_T(\infty) \approx -R_o/R_p \quad (30)$$

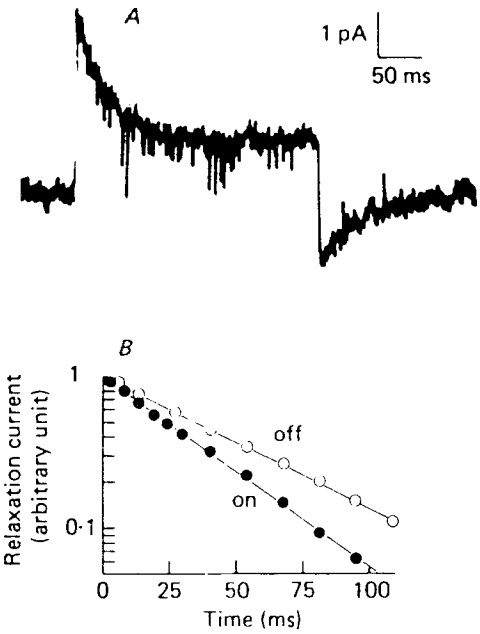

Fig. 8. An example of the distortion of an experimental single channel current record (*A*) occurring in a small cell to demonstrate the measurement of the 'on' and 'off' current relaxation time constants (τ_{on} and τ_{off}) plotted semi-logarithmically in (*B*). τ_{on} and τ_{off} were measured to be 36 and 51 msec, respectively. R_o and R_p were estimated using Eqs. (28) and (29) to be 30 and 26 GΩ, respectively. Both panels were reproduced from Fenwick et al. (1982) with permission. *See* that paper for further details

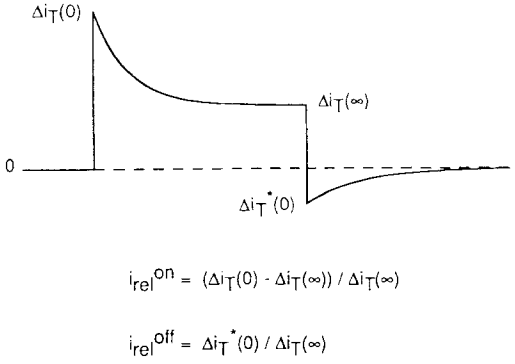

Fig. 9. An illustration of the method of calculating i_{rel}^{on} and i_{rel}^{off}. All parameters are measured with respect to the current baseline (dashed line). $\Delta i_T(\infty)$ must be measured only after the open channel current has reached a steady state. i_{rel}^{on} represents the initial fractional increase in current relative to the steady-state value towards the end of a long channel opening and i_{rel}^{off} represents the immediate fractional value of current just after channel closure, again relative to the (on) steady-state value of current

$$i_{rel}^{on} \equiv [\Delta i_T(0) - \Delta i_T(\infty)]/\Delta i_T(\infty) \approx R_o/R_p + R_o\gamma_c \quad (31)$$

where i_{rel}^{off} and i_{rel}^{on} are measured as shown in Fig. 9 (*see also* the Appendix); $\Delta i_T(0)$ and $\Delta i_T(\infty)$ represent the currents at the beginning and end of a long chan-

nel opening; $\Delta i_T^*(0)$ represents the peak value of current just after the channel has closed and γ_c is the channel conductance in excised patches. If only the apparent cell-attached conductance γ_{app} is known, the corrected conductance can be calculated using Eqs. (27) and (30). For larger values of C_p/C_o, however, slightly more complicated equations [e.g., Eqs. (A34) and (A33)] will have to be used. The absence of large negative relaxations suggests relatively high values for R_p [and/or C_p; Eq. (A34)], implying minimal damage caused to the patch membrane by the cell-attached pipette (Fenwick et al., 1982).

In the symmetrical case, where $C_p/C_o \approx R_o/R_p$, $i_{rel}^{off} \approx 0$ [Eq. (A36)]. This condition implies that the patch conductance has exactly the share of total conductance that would be predicted from its size (as indicated by its capacitance). In such a case, the membrane recharging process following channel closure would be electrically silent (the resistive component resulting from current across the patch being exactly balanced by the capacitative one). In contrast, if $C_p/C_o \approx 0$ and R_o/R_p is significant (*see also* above), a condition representing the case in which there is a negligible capacitative component but finite patch conductance, a negative tail current will be generated. The difference between these two predictions underlines the sensitivity of i_{rel}^{off} to the difference between C_p/C_o and δ [*see* Eq. (A34)]. This difference is likely to vary considerably from one membrane patch to another and hence will tend to result in a variable channel closure response from one cell to the next.

In practice, these types of analysis give only approximate estimates of R_o and R_p. Some scatter normally occurs with τ_{on} and τ_{off}, and i_{rel}^{on} and i_{rel}^{off}, presumably because of variations in R_o, caused by channels opening and closing elsewhere in the cell. Accordingly, the larger measured values of τ_{on} and τ_{off} and of i_{rel}^{on} and i_{rel}^{off}, with a minimal number of additional open channels, probably give the more accurate estimate of R_o. It is also important to recognise that when positive pipette potentials are used, the membrane potential may be significantly depolarized and the measured R_o may be significantly less than the value of R_o valid near the normal resting potential of the cell.

Corrections for Intact-Patch Single-channel Conductance and Reversal Potential Measurements

Given that a reasonable estimate of R_o/R_p has been made and that approximate estimates of C_o and C_p can be deduced, it is possible to correct the apparent measurements of single-channel conductance τ_{app} and E_{app} to obtain good estimates of the actual γ_c and E_c values. The apparent single-channel slope conductance, γ_{app}, may be obtained from Eqs. (20)–(22). In the Appendix, it is then shown that for small cells the correct value of single-channel slope conductance γ_c is related to the apparent value by

$$\gamma_c = \gamma_{app}(1 + \delta)(1 + C_p/C_o) \tag{32}$$

where $\delta = R_o/R_p$. If $C_p/C_o \ll 1$, this simplifies even more to

$$\boldsymbol{\gamma_c = \gamma_{app}(1 + \delta).} \tag{33}$$

The real reversal potential, E_c, is then related to the apparent one, E_{app}, by

$$E_c = (E_{app} + E_p\delta)/(1 + \delta). \tag{34}$$

If $E_p \approx 0$ (as would be expected with a pipette solution of 150 mM KCl), Eq. (34) simplifies even more to

$$\boldsymbol{E_c = E_{app}/(1 + \delta).} \tag{35}$$

For example, for mammalian olfactory receptor neurons, uncorrected estimates of channel conductance and null potential [using Eqs. (20) and (21)], from intact patch measurements, were shown to be in error by about 35% (Lynch & Barry, 1989) when compared to values correctly evaluated using Eqs. (32) and (34) or when compared to excised patch measurements. For example, the corrected single-channel conductance value for one particular channel measured was 29 pS, compared to an uncorrected value of 19 pS, and the corrected reversal potential was −44 mV, compared to an uncorrected value of −60 mV.

Junction Potential Corrections and Small Cell Effects

In order to also correct for any liquid junction potentials, it is merely necessary to substitute $(V_P - E_L)$ for V_P in Eq. (20) or $(V_P^o - E_L)$ for V_P^o in Eq. (21), where E_L is the liquid junction potential (solution − pipette) as shown in Fig. 2 [*cf.* Eq. (5)].

Summary and Concluding Remarks

1) In patch-clamp measurements, with the pipette solutions comparable in concentration to the bathing solution and containing ions with low mobilities,

liquid junction potential contributions may be up to 10 mV, or possibly even more, in magnitude. Although the patch-clamp technique may appear to eliminate junction potentials, they are almost invariably present in all configurations and must be taken into account for accurate measurements. Equations and procedures for estimating the junction potentials and rules for using them to correct measurements have been outlined.

2) In small cells, where the input resistance of the cell is not very much less than the seal resistance, a significant fraction of the recorded current can be leaking through the seal resistance. Various techniques have been suggested to enable the input resistance of small cells to be estimated under certain conditions, for both intact-patch and whole-cell measurements.

3) In small cells, the current passing through a channel in an intact patch can radically change the potential in the cell and so alter the driving force across the patch for that current. This can result in a very distorted current waveform and, under certain conditions, can even initiate an action potential elsewhere in the cell. It can also invariably result in large errors (e.g., 30% in one set of cited measurements) in estimates of single-channel conductance and channel reversal potential. A full circuit analysis has been presented to model this effect and to enable true values of single-channel conductance and channel reversal potential to be obtained from the apparent measured values. In addition, the analysis shows how various other cell parameters may also be evaluated from the experimental measurements of the distorted current waveforms.

We would especially like to thank Professor Neher for his critical reading of the manuscript and helpful comments.

This work was supported by the Australian Research Council and the National Health and Medical Research Council of Australia.

References

Ammann, D. 1986. Ion-Selective Microelectrodes. Springer-Verlag, Berlin

Ashcroft, F.M., Harrison, D.E., Ashcroft, S.J.H. 1984. *Nature* **312:**446–448

Atwater, I., Rosario, L., Rojas, E. 1983. *Cell Calcium* **4:**451–461

Barry, P.H. 1989. *Meth. Enzymol.* **171:**678–715

Barry, P.H., Diamond, J.M. 1970. *J. Membrane Biol.* **3:**93–122

Cahalan, M.D., Chandy, K.G., DeCoursey, T.E., Gupta, S. 1985. *J. Physiol.* **358:**197–237

Caldwell, P.C. 1968. *Int. Rev. Cytol.* **24:**345–371

Dean, J.A. 1985. Lange's Handbook of Chemistry. J.A. Dean, editor. (13th ed.) McGraw-Hill, New York

Dionne, V.E. 1989. *In:* Chemical Senses. Vol. 1, pp. 415–426. J.H. Teeter and M.R. Kare, editors. Marcel Dekker, New York

Fenwick, E.M., Marty, A. Neher, E. 1982. *J. Physiol.* **331:**577–597

Fernandez, J.M., Fox, A.P., Krasne, S. 1984. *J. Physiol.* **356:**565–585

Firestein, S., Werblin, F.S. 1987. *Proc. Natl. Acad. Sci. USA* **84:**6292–6296

Fischmeister, R., Ayer, R.K., DeHaan, R.L. 1986. *Pfluegers Arch.* **406:**73–82

Frings, S., Lindemann, B. 1988. *J. Membrane Biol.* **105:**233–243

Hamill, O.P., Marty, A., Neher, E., Sakmann, B., Sigworth, F.J. 1981. *Pfluegers Arch.* **391:**85–100

Kehl, S.J., McBurney, R.N. 1989. *Neuroscience* **33:**579–586

Lynch, J.W., Barry, P.H. 1989. *Biophys. J.* **55:**755–768

Lynch, J.W., Barry, P.H. 1991. *J. Gen. Physiol.* (*in press*)

MacInnes, D.A. 1961. The Principles of Electrochemistry. Dover, New York

Marty, A., Neher, E. 1983. *In:* Single-Channel Recording. B. Sakmann and E. Neher, editors. pp. 107–122. Plenum, New York

Maue, R.A., Dionne, V.E. 1987. *J. Gen. Physiol.* **90:**95–125

Meier, P.C., Ammann, D., Morf, W.E., Simon, W. 1980. *In:* Medical and Biomedical Applications of Electrochemical Devices. J. Koryta, editor. pp. 13–91. John Wiley & Sons, New York

Morf, W.E. 1981. The Principles of Ion-Selective Electrodes and of Membrane Transport. Elsevier, Amsterdam—New York

Neher, E. 1991. *In:* Ion Channels. *Meth. Enzymol.* (*in press*)

Neher, E., Sakmann, B., Steinbach, J.H. 1978. *Pfluegers Arch.* **375:**219–228

Page, K.R. 1980. *Comp. Biochem. Physiol.* **67A:**637–642

Pusch, M., Neher, E. 1988. *Pfluegers Arch.* **411:**204–211

Robinson, R.A., Stokes, R.H. 1965. Electrolyte Solutions. (2nd ed., revised) Butterworths, London

Rorsman, P., Trube, G. 1986. *J. Physiol.* **372:**405–423

Sakmann, B., Neher, E. 1983. *In:* Single-Channel Recording. B. Sakmann and E. Neher, editors. pp. 37–51. Plenum, New York

Schild, D. 1989. *Exp. Brain Res.* **78:**223–232

Serway, R.A. 1986. Physics for Scientists and Engineers. (2nd ed.) Saunders College Publishing, New York

Sigworth, F.J. 1983. *In:* Single-Channel Recording. B. Sakmann and E. Neher, editors. pp. 3–35. Plenum, New York

Suzuki, N. 1989. *In:* Chemical Senses. Vol. 1, pp. 469–493. J.H. Teeter and M.R. Kare, editors. Marcel Dekker, New York

Trotier, D. 1986. *Pfluegers Arch* **407:**589–595

Trotier, D., Rosin, J.-F., MacLeod, P. 1989. *In:* Chemical Senses. Vol. 1, pp. 427–448. J.H. Teeter and M.R. Kare, editors. Marcel Dekker, New York

Weast, R.C. 1980. Handbook of Chemistry and Physics. (61st ed.) R.C. Weast, editor. CRC, Boca Raton, FL

Received 25 July 1990; revised 3 December 1990

Appendix

Solution of Equations Describing Current Flow during the Opening and Closure of a Single Channel in an Intact Membrane Patch on a Small Cell

The electrical circuit will be assumed to be as shown in Fig. 6. The first part of the analysis in this appendix [from the opening of the channel up to Eq. (A19)] summarizes the derivation outlined in Appendix A of Lynch and Barry (1989). The second part of the derivation is new [the steady-state response and the closure of the channel, from Eq. (A20) on]. As already noted (*see* Footnote 3, pp. 106), in order to make the equations and derivation more readable and uniform, the previous parameters E_m and E_p of Lynch and Barry are now redefined as E_o and E_p, respectively.

Before the Channel Opens

In the steady-state before the channel opens, the total background current i_T^b is given by

$$i_T^b = (V_i - E_p - V_P)/R_p + (i_s) \tag{A1}$$

$$i_T^b = (E_o - V_i)/R_o + (i_s) \tag{A2}$$

where V_i represents the potential of cell interior with respect to external solution (Fig. 5; equivalent to V in Lynch & Barry, 1989); E_p represents the diffusion potential for the remainder of the membrane patch; V_P the pipette potential; E_o the resting potential of the cell in the absence of any current flow; R_p is the resistance of the patch (excluding the channel) and R_o is the resistance of the rest of the cell. From this point on, i_s, the current through the seal resistance [$i_s = (E_s - V_P)/R_s$] will be ignored and the term dropped, since it is a constant term that will cancel out in the later equations. From the above equations, it may be seen that the initial cell potential, V_i^b, before the channel opens is given by

$$V_i^b = [E_o + E_p\delta + V_P\delta]/[1 + \delta] \tag{A3}$$

and

$$i_T^b = -[V_P + E_p - E_o]/[R_p(1 + \delta)] \tag{A4}$$

with

$$\delta \equiv R_o/R_p \tag{A5}$$

where δ represents the ratio of cell-to-patch resistance, a critical parameter that is a measure of the relative size of the cell and which tends to zero as the size of the cell increases.

Opening of the Channel ($t \geq 0$; Neglecting i_s)

At any time t after the opening of the channel, the total current i_T will be given by

$$i_T = C_p\frac{d(V_i - V_P)}{dt} + \frac{(V_i - E_p - V_P)}{R_p} + \frac{(V_i - E_c - V_P)}{R_c} \tag{A6}$$

and

$$i_T = -C_o\frac{dV_i}{dt} + \frac{(E_o - V_i)}{R_o} \tag{A7}$$

where C_p and C_o represent the capacitances of the patch and the rest of the cell; E_c and R_c the reversal potential (null potential) and resistance of the channel, respectively, and i_T represents the total current flowing across the patch and cell (excluding i_s, the current flowing through the leakage pathway). Equations (A6) and (A7) may be combined and rearranged to give

$$\tau\frac{dV_i}{dt} + (1 + \delta + \beta)V_i - [E_o + (E_p + V_P)\delta + (E_c + V_P)\beta] = 0 \tag{A8}$$

where

$$\tau \equiv R_o(C_o + C_p) \tag{A9}$$

and

$$\beta \equiv R_o/R_c \tag{A10}$$

defining

$$\alpha \equiv \delta + \beta. \tag{A11}$$

Solving Eq. (A8), with the condition that when $t = 0$, $V_i = V_i^b$ (from Eq. A3),

$$V_i(t) = \frac{[E_o + E_p\delta + E_c\beta + V_P\alpha]}{[1 + \alpha]} - \frac{\beta[V_P - E_o - E_p\delta + (1 + \delta)E_c]}{[1 + \alpha][1 + \delta]}e^{-(1+\alpha)t/\tau}. \tag{A12}$$

The *change in cell potential* during the opening of the channel [*cf.* Eqs. (A18)–(A21) of Lynch & Barry, 1989] is then given by

$$\Delta V_i(t) = V_i(t) - V_i^b = \theta[1 - e^{-(1+\alpha)t/\tau}] \tag{A13}$$

where

$$\theta = \frac{\beta[V_P - E_o - E_p\delta + (1 + \delta)E_c]}{[1 + \alpha][1 + \delta]}. \tag{A14}$$

The change in current during the opening of the channel, Δi_T, is given by

$$\Delta i_T \equiv i_T - i_T^b \tag{A15}$$

and may be shown to be given by

$$\Delta i_T = -(\theta/R_o)\{1 - [1 - (1 + \alpha)R_oC_o/\tau]e^{-(1+\alpha)t/\tau}\} \tag{A16}$$

which is the same as Eq. (A25) of Lynch and Barry (1989). When $t = 0$, the peak value of the current $\Delta i_T(0)$ is given by

$$\Delta i_T(0) = -\gamma_c[(V_P - E_o - E_p\delta)/(1 + \delta) + E_c] \cdot [C_o/(C_o + C_p)] \tag{A17}$$

where

$$\gamma_c \equiv 1/R_c. \tag{A18}$$

For large cells, in which case $\delta \rightarrow 0$ and $C_p/C_o \rightarrow 0$ [*cf.* Eq. (A27) of Lynch & Barry, 1989]

$$\Delta i_T(0) = -\gamma_c(V_P - E_o + E_c). \tag{A19}$$

Steady-State Current Response

For a very long channel opening, the current will reach a steady-state value $\Delta i_T(\infty)$, which will be given by

$$\Delta i_T(\infty) = -[\theta/R_o] = -\gamma_c[V_P - E_o - E_p\delta + (1 + \delta)E_c]/[(1 + \alpha)(1 + \delta)] \tag{A20}$$

and

$$V_i(\infty) = [E_o + E_p\delta + E_c\beta + V_P\alpha]/[1 + \alpha]. \tag{A21}$$

Closure of the Channel

The differential equations describing the *closure* of the channel are

$$i_T = C_p\frac{d(V_i - V_P)}{dt} + \frac{(V_i - E_p - V_p)}{R_p} \tag{A22}$$

$$i_T = -C_o\frac{dV_i}{dt} + \frac{(E_o - V_i)}{R_o}. \tag{A23}$$

The general solution of the Eqs. (A22) and (A23), following a voltage V_i^o at the end of the channel opening V_i^o, is given by

$$V_i(t) = \frac{[E_o + \delta(E_p + V_P)] + \{V_i^o[1 + \delta] - [E_o + \delta(E_p + V_P)]\}}{[1 + \delta]} \cdot e^{-(1+\delta)t/\tau}. \tag{A24}$$

Channel Closure After a Long Opening

After a long channel opening in which it can be assumed that $V_i^o = V_i(\infty)$, it can readily be shown from Eqs. (A24) and (A21) that in terms of a new time scale, where t now represents the time *after* the closure of the channel, that V_i is given by

$$V_i = [E_o + \delta(E_p + V_P)]/[1 + \delta] + \theta e^{-(1+\delta)t/\tau}. \tag{A25}$$

From Eq. (A23), the change in current above the base line level ($\Delta i_T = i_T - i_T^b$) may be shown to be given by

$$\Delta i_T(t) = -(\theta/R_o)\{1 - (1 + \delta)[C_o/(C_o + C_p)]\}e^{-(1+\delta)t/\tau} \tag{A26}$$

where θ/R_o is given [*see* Eq. (A14)] by

$$\theta/R_o = \gamma_c\frac{[V_P - E_o - E_p\delta + (1 + \delta)E_c]}{[1 + \alpha][1 + \delta]}. \tag{A27}$$

Time Constants for Current Relaxation during Channel Opening and Closure

From Eq. (A16), the time constant for the relaxation of current during the channel opening, τ_{on}, will be given by

$$\tau_{on} = \tau/(1 + \alpha) = R_o(C_o + C_p)/(1 + \alpha). \tag{A28}$$

Similarly, the time constant for the relaxation of current during the channel closure, τ_{off}, will be given by

$$\tau_{off} = \tau/(1 + \delta) = R_o(C_o + C_p)/(1 + R_o/R_p). \tag{A29}$$

From Eqs. (A28) and (A29), it may be shown that

$$(\tau_{off}/\tau_{on}) - 1 = \beta/(1 + \delta) = (R_o/R_c)/(1 + R_o/R_p). \tag{A30}$$

Peak Current Drifts

A comparison of the proportionate change in peak current at the opening and closure of the channel, relative to the steady-state current level can also yield some interesting information. Refer also to Fig. 9 for definitions. Defining i_{rel}^{on} by

$$i_{rel}^{on} \equiv [\Delta i_T(0) - \Delta i_T(\infty)]/\Delta i_T(\infty) \tag{A31}$$

where $\Delta i_T(0)$ represents the peak current at the opening of the channel [Eq. (A17)] and $\Delta i_T(\infty)$ represents the final 'steady-state' level of current reached, provided the channel opening is sufficiently long [Eq. (A21)]. Similarly, after channel closure, i_{rel}^{off} will be defined by

$$i_{rel}^{off} \equiv \Delta i_T^*(0)/\Delta i_T(\infty) \tag{A32}$$

where $\Delta i_T^*(0)$ represents the peak current immediately following channel closure.

From Eqs. (A17) and (A21), it may be readily deduced that

$$i_{rel}^{on} = [\delta + \beta - (C_p/C_o)]/[1 + (C_p/C_o)]. \tag{A33}$$

Similarly from Eqs. (A26) and (A27), it may be readily shown that

$$i_{rel}^{off} = [(C_p/C_o) - \delta]/[1 + (C_p/C_o)]. \tag{A34}$$

It should be noted that in the symmetrical case (*see* Discussion), if $C_p/C_o \approx R_o/R_p = \delta$, that Eqs. (A33) and (A34) simplify to

$$i_{rel}^{on} = \beta/(1 + \delta) \tag{A35}$$

and

$$i_{rel}^{off} \approx 0. \tag{A36}$$

Alternatively, if $C_p/C_o \approx 0$ and δ is significant, then

$$i_{rel}^{on} \approx \delta + \beta = R_o/R_p + R_o/R_c \tag{A37}$$

and

$$i_{rel}^{off} \approx -\delta = -R_o/R_p. \tag{A38}$$

The dissimilarity between Eqs. (A36) and (A38) indicate how sensitive i_{rel}^{off} is to the difference between C_p/C_o and δ. This difference is likely to vary considerably from one membrane patch to another and hence will tend to result in a very variable channel closure response from one cell to the next.

Corrections to Single-Channel Conductance

From an inspection of Eq. (A17), the measured (apparent) slope conductance, γ_{app}, obtained using the initial peak values of the current $[\Delta i_T(0)]$ from $d(\Delta i_T(0))/dV_P$, will be given by

$$\gamma^0_{app} = \gamma_c/[(1 + \delta)(1 + C_p/C_o)]. \tag{A39}$$

If C_p/C_o is very small, then

$$\gamma^0_{app} \approx \gamma_c/(1 + \delta). \tag{A40}$$

If the steady-state value of the current were to be used, then from Eq. (A20), $\gamma^\infty_{app} = d(\Delta i_T(\infty))/dV_P$, will be given by

$$\gamma^\infty_{app} = \gamma_c/[(1 + \delta)(1 + \delta + \beta)]. \tag{A41}$$

Correction to Reversal Potential Measurements

If V^o_P represents the pipette potential at which the initial peak single-channel current $\Delta i_T(0) = 0$, then from Eq. (A17)

$$(V^o_P - E_o - E_p\delta)/(1 + \delta) + E_c = 0. \tag{A42}$$

Defining the apparent reversal potential as E^*_c by

$$E^*_c \equiv E_o - V^o_P \tag{A43}$$

it may readily be shown from Eqs. (A42) and (A43) that

$$E_c = (E^*_c + E_p\delta)/(1 + \delta). \tag{A44}$$

If $E_p \approx 0$ (with 150 mM KCl in the pipette and no significant anion permeability in the patch), Eq. (A40) simplifies to

$$E_c = E^*_c/(1 + \delta). \tag{A45}$$

Computer Program for Plotting Single-Channel Waveforms

A computer program in Turbo C (Borland International) has been written for IBM-PC compatible computers to plot current waveforms for single-channel openings in membrane patches in small cells. The program uses Eqs. (A16), (A26) and (A27) and associated equations and, given a set of cell parameters, will plot the resulting current waveform on both computer screen and either an HP plotter or HP LaserJet printer. It was used to generate Figs. 7 and 9. Further details are available from PHB.